Int. J. Electrochem. Sci., 15 **(2020)** 4900 – 4907, doi: 10.20964/2020.06.29

International Journal of
ELECTROCHEMICAL
SCIENCE
www.electrochemsci.org

Short Communication

Effect of hydrogen induced decrepitation on the hydrogen sorption properties of $MmNi_5$

St. Todorova, V. Rangelova, L. Mihaylov, T. Spassov[*]

Sofia University "St. Kl. Ohridski", Faculty of Chemistry and Pharmacy, 1 James Bourchier Blvd. 1164 Sofia, Bulgaria
[*]E-mail: tspassov@chem.uni-sofia.bg

Received: 5 February 2020 / *Accepted:* 10 March 2020 / *Published:* 10 May 2020

$MmNi_5$ hydrogen storage alloy with an average particle size of 120 μm was subjected to hydriding treatment at 50°C, under 40 atm. pure hydrogen atmosphere. As a result, a large density of particle cracks was formed, which led to an increase in the particle surface area. The enlarged particles surface, in turn, led to substantially improved hydrogen sorption kinetics compared to the as-received (untreated) alloy. It was also found that hydrogen-induced decrepitation of the $MmNi_5$ powder results in enhancement of the hydrogen diffusivity mainly due to shortening of its diffusion distances.

Keywords: $MmNi_5$, hydrogen storage, hydriding kinetics, H-induced decrepitation

1. INTRODUCTION

Among all hydrogen storage alloys, rear earth AB_5 - type is still one of the most studied since its large scale industrial production and commercialization. About 10 % of the rear earth production is used in Ni - MH batteries manufacturing. They are still hardly replaceable in the automotive industry for powering hybrid car electric motors because of their safe operation and long life [1]. $LaNi_5$ being one of the most studied intermetallics in this group has promising hydrogen storage characteristics both from gas phase and electrochemically – absorbs about 1.5 wt % H_2 with low plateau pressure in the p-c diagrams and has an electrochemical capacity of 372 mAh/g [2]. However, its cost is relatively high and the hydriding - dehydriding cycling leads to fast degradation of its crystal structure in gas phase due to lattice deformations and corrosive degradation in solution [3]. Improvement in $LaNi_5$ alloys performance is possible by substituting La by mischmetal (Mm), thus reducing the content of La and increasing the content of other rear earths – Ce, Pr, Nd. The influence of Ce content on the overall performance of the alloys is studied in many publications showing that replacing La with certain

amounts of Ce leads to an increase in the plateau pressure and lattice expansion in gas phase sorption. In electrochemical cycling, it has a positive effect on corrosion suppression due to protective oxide film formation [3-6]. Thus, $MmNi_5$ characterizes with lower charge capacity, but better stability in the electrode performance.

Successful attempts to improve the hydrogen-sorption characteristics of $MmNi_5$ (lower absorption pressure and improved hydriding kinetics) consist mainly in (i) alloying (Al, Mn, Co, Fe), (ii) formation of composites based on $MmNi_5$, (iii) particle and crystallite size reduction, achieved mainly by ball milling. The substitution of Ni by other transitional metals in the crystal lattice is a popular approach to modify the crystal structure and improve the hydrogen storage properties of $MmNi_5$ [7, 8]. Alloying of $MmNi_5$ with other transitional metals (like Pt, Pd, Co, Ni, Fe, Mn) mainly through ball milling is a useful approach adopted from AB_2 type materials. The addition of small amounts of transitional metals does not change the crystal structure rather acts as a catalyst and eases the process of dissociation of hydrogen molecule into atoms on the alloy surface and their subsequent diffusion in the crystal lattice [9, 10].

Reducing the size of the particles and crystallites is another way to increase the active surface of the materials used for hydrogen storage and modify their microstructure. It has the same effect in the case of $MmNi_5$ alloy – enhanced absorption-desorption kinetics at lower temperature and pressure [11, 12]. However, extreme reduction of crystallite size usually leads to deformations in the crystal structure of AB_5-type alloys, and a reduction of the hydrogen storage capacity is observed [12]. The present work aims at reducing the $MmNi_5$ particle size using a different approach – hydrogen-induced decrepitation (50˚C, 40 atm H_2) and thus improving its hydrogen sorption kinetics characteristics.

2. EXPERIMENTAL

$MmNi_5$ alloy (Sigma-Aldrich Product № 685976) was used in the present study. The as-received $MmNi_5$ powder was subjected to hydriding at 50 ^oC under 40 bar pure hydrogen atmosphere and subsequent dehydriding at 50 ^oC and 1 bar H_2 to achieve hydrogen-induced particles decrepitation. The structure of the alloy before and after hydrogen-induced decrepitation was determined using XRD (Cu-K_α radiation). The morphology and size of the particles were characterized using scanning electron microscope JEOL 5510.

Hydrogenation kinetic curves of the samples were measured by a Sieverts'-type apparatus (PCT) at room temperature. To determine the hydrogen diffusion coefficient in the as-received and decrepitated $MmNi_5$ alloys, the samples were charged electrochemically under galvanostatic conditions using a three-electrode cell. The working electrode was prepared using a mixture of 70 mg of the alloy, 100 mg teflonized carbon and heptane, subsequently pressed at about 150 atm to form the electrode and left on air to dry. $NiOOH/Ni(OH)_2$ was used as a counter electrode and Ag/AgCl as reference. The electrolyte was 6 M KOH water solution. Each electrode is charged for 3 hours at 5mA. Then the hydrogen charged samples were discharged at potentiostatic conditions (900 mV) in the same electrolyte. The discharge potential was selected to correspond to the discharge potential plateau from the galvanostatic charge/discharge experiments [13].

3. RESULTS AND DISCUSSION

The as-received and hydrogen treated (at 50°C and 40 bar H_2) $MmNi_5$ alloys reveal similar particle shape and size, Fig. 1. The average particle size of about 120 μm was determined for the initial alloy and a little lower value for the treated sample (~ 100 μm) (fig.1). A significant difference in the morphology of the particles is, however, observed at higher magnification. The powder particles after H-treatment contain a large number of cracks, well visible on their surface. Thus, it was proved that under the applied hydriding conditions (50°C, 40 bar H_2) the $MmNi_5$ powder particles undergo cracking due to the intense absorption and accumulation of hydrogen in the crystal lattice of the compound, thus leading to mechanical stress in the alloy. This effect is known for AB_5-type and Ti-V based alloys, but for much larger particles, in which case the powder particles are fragmented to micron size [14, 15, 16]. The interesting result in the present study is that this effect (H-induced decrepitation) is also achieved with smaller particles under rather moderate conditions. It is known that a number of hydrogen storage alloys undergo pulverization (decrepitation) during hydriding/dehydriding from a hydrogen gas phase [14, 17, 18] and during electrochemical hydrogen charge/discharge [15, 16]. The pulverization mechanism for some hydrogen storage alloys has been clarified [14, 15, 16], but there is still a need to study its influence on the alloys hydriding properties.

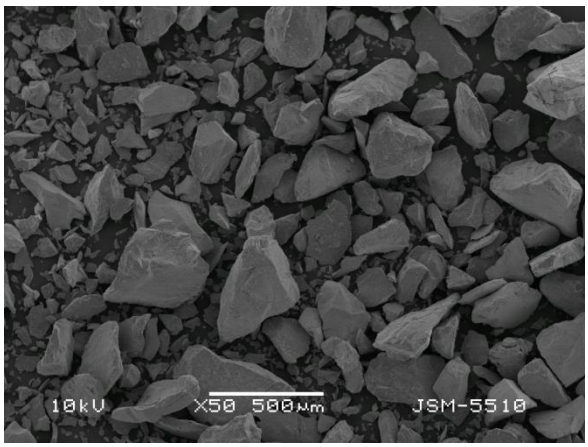

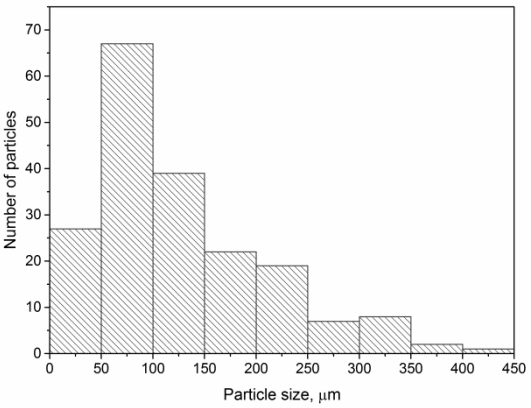

(a)

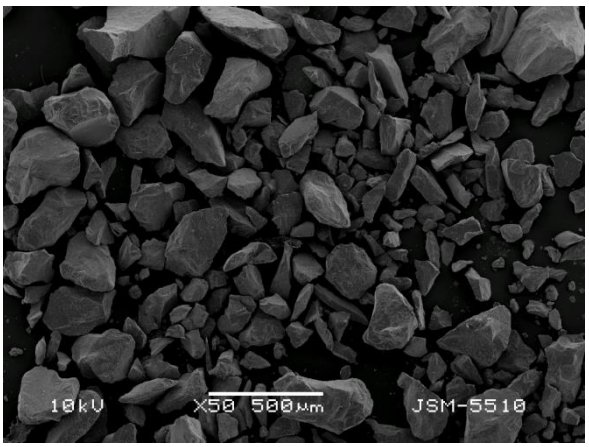

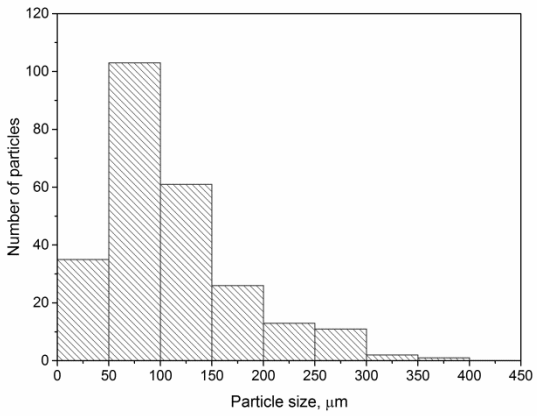

(b)

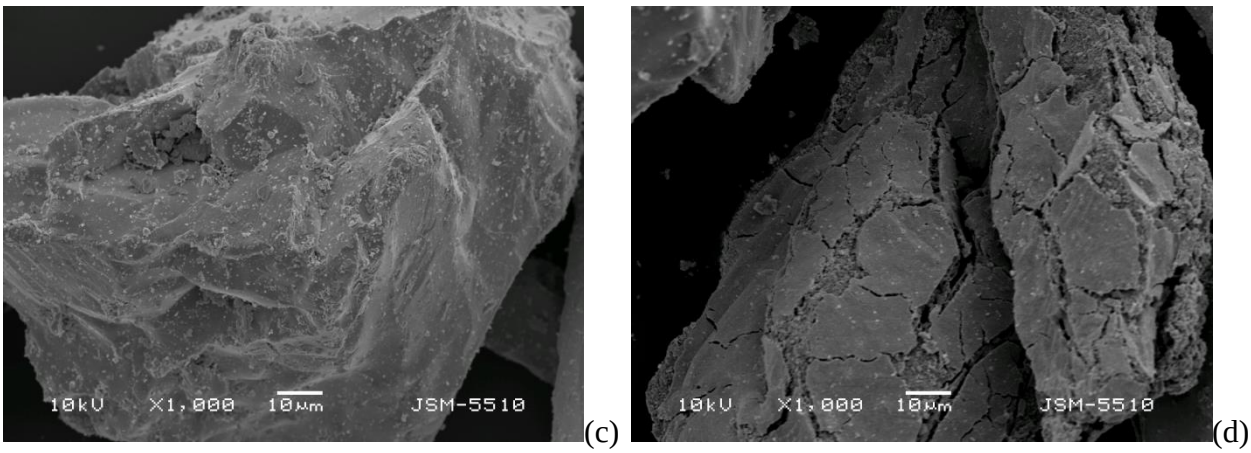

(c) (d)

Figure 1. SEM micrographs of as-received (a, c) and decrepitated (b, d) $MmNi_5$ and particle size distribution histograms of both samples.

The XRD analysis also shows some differences between the as-received and hydrogen treated $MmNi_5$ alloys (ht-$MmNi_5$), Fig. 2. The diffraction peaks of both samples correspond to the hex. $LaNi_5$ compound with some shift in the peak positions due to the partial substitution of Ce for La in $LaNi_5$. The diffraction peaks of the H-decrepitated sample show a little decrease in intensity and an increase in width. Preliminary hydrogenation at a higher temperature and hydrogen pressure causes mainly particle cracking and in a much smaller degree leads to microstructural changes, associated with grain refinement and introduction of crystal lattice stresses.

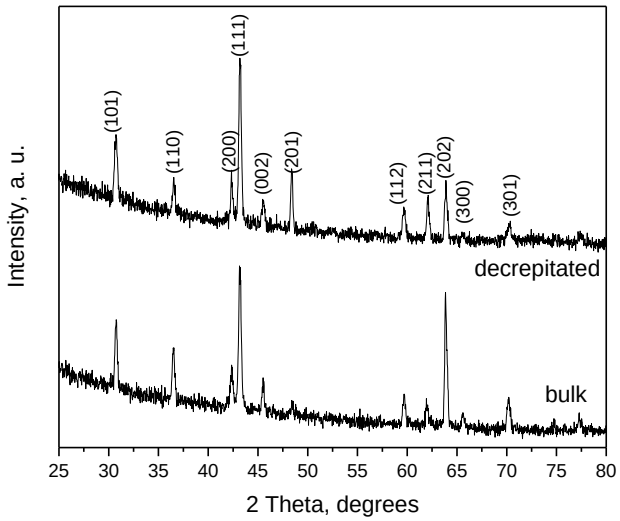

Figure 2. X-ray diffraction patterns of as-received and heat-treated in H_2 atmosphere (50°C, 40 bar H_2) $MmNi_5$.

Hydrogen absorption kinetic curves of the as-received $MmNi_5$ powder and hydrogen decrepitated $MmNi_5$ sample, measured during the third cycle are presented in Fig. 3. The as-received $MmNi_5$ powder shows only limited hydrogen uptake; the absorption capacity reaches only about 0.5 wt.% hydrogen for about an hour. The rather low sorption capacity of the as-received sample is

probably due to relatively slow hydrogen sorption kinetics under the applied experimental conditions (25 atm., 20ºC). The decrepitated sample shows substantially better absorption kinetics and hydrogen capacity, revealing 1.4 wt.% H_2 for 30 min. Undoubtedly, the observed significant difference in the kinetics of hydrogen sorption and hydrogen capacity between the two samples must be related to the more highly developed surface of the powder after hydrogen-induced decrepitation (Fig.1). Apparently, the higher rate of H-absorption is due mainly to the increased particle surface area (presence of cracks and removed surface oxide layer) and to a lesser extent to generated stresses in the crystal lattice of the material after decrepitation.

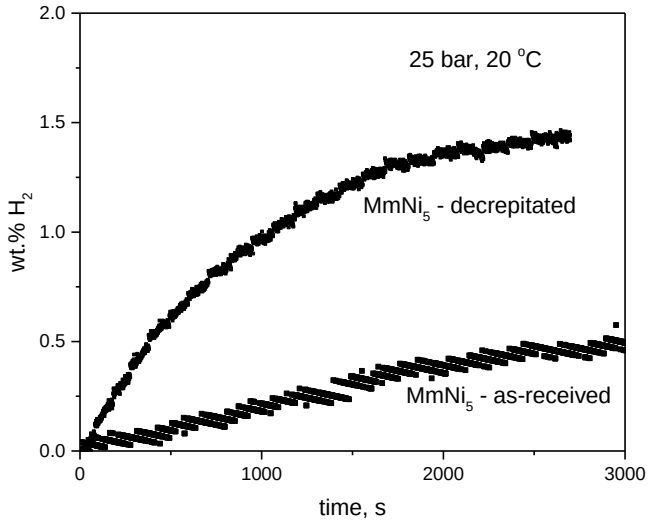

Figure 3. Hydrogen absorption curves for as-received and decrepitated $MmNi_5$ at 20ºC and 25 bar H_2.

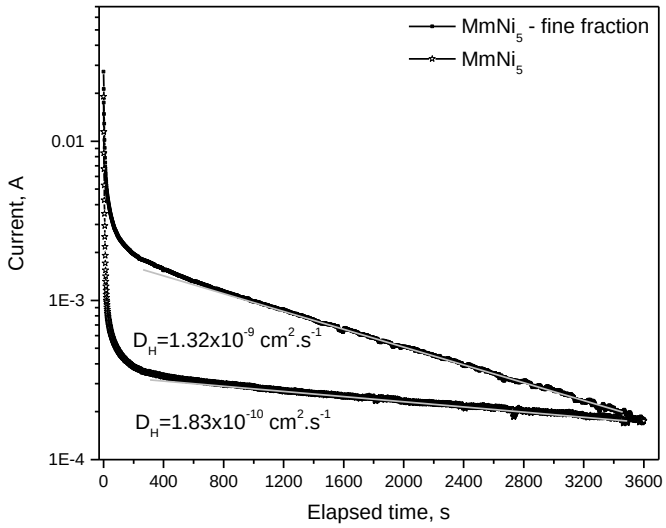

Figure 4. "lg(J_H) vs. discharge time t", during potentiostatic discharge of $MmNi_5$: as-received sample and after hydrogen-induced decrepitation.

An additional and independent way to evaluate the rate of hydrogen sorption and diffusion mobility of hydrogen in the studied alloys is the electrochemical potentiostatic discharge of initially hydrogen charged samples.

Fig. 4 compares hydrogen discharge curves of as-received and hydrogen treated alloys in coordinates "ln(J_H) vs. discharge time t". Thus, applying the following approximation for the current density [19]:

$$J_H = \frac{(c_0 - c^*)D_H}{L^2} \exp\left(-\frac{\pi^2 D_H t}{4L^2}\right), \qquad \text{(Eq. 1)}$$

the diffusion coefficients of hydrogen into $MmNi_5$ particles were determined. In the above equation, J_H is the current density, t is the discharge time, D_H is the hydrogen diffusion coefficient, L is the size of the particles (average particle size, which is 120 μm for the alloys studied), c_o is the initial hydrogen concentration, c* is the hydrogen concentration after the electrode is anodically biased. From the slope of the plot "ln(J_H) vs. t", Fig. 4, hydrogen diffusion coefficient $D_H = 2.1 .10^{-12}$ $cm^2.s^{-1}$ has been determined for the as-received $MmNi_5$ alloy. The D_H value determined for the as-received $MmNi_5$ is somehow lower compared to those obtained by other authors for similar alloys [20-26]. It needs, however, to be mentioned that the diffusion coefficients of hydrogen vary in a large range between 10^{-8} and 10^{-11} $cm^2.s^{-1}$, mainly due to the different methods used for their estimation, but also because of the differences in the microstructure of the alloys (defects, grain size, etc.). Therefore, in the present work, the goal was to compare the D_H of both studied alloys providing the same experimental conditions of potentiostatic discharge, Fig. 4. Indeed, the discharge curves reveal a substantially higher rate of discharge of the decrepitated alloy (further in the text ht-$MmNi_5$) compared to the as-received material. This result could be explained in two ways (i) the diffusion coefficient of the ht-$MmNi_5$ alloy is essentially higher, due to the microstructural changes result of the treatment and (ii) presence of shorter diffusion distances due to the formed cracks and other defects. As the XRD analysis does not show large deviations in the grain size and defects concentration upon the hydrogen treatment, the same D_H for both alloys could be assumed. Thus applying eq. (1) one can determine the effective size of the powder particles. From the slope of the hydrogen discharge curve of the ht-$MmNi_5$, using the D_H for the initial $MmNi_5$ alloy an average diffusion distance of 35 μm was obtained. That value can be considered as an effective size of the powder particles for ht-$MmNi_5$.

4. CONCLUSIONS

The study shows the effect of primary hydrogen-induced depreciation on the H-sorption properties of $MmNi_5$ hydrogen storage alloy. Hydrogenation at 50°C and 40 bar hydrogen has been found to result in the formation of a large number of particles cracks and, therefore, to a more developed particle surface favoring the kinetics of hydrogenation at room temperature.

It was also proved that the accelerated hydrogen sorption (and higher diffusion coefficient respectively) is not a consequence of changes in the $MmNi_5$ crystal lattice, but mainly of shortening in the diffusion distances of the hydrogen atoms resulting from the particle cracking.

ACKNOWLEDGEMENT
The experiments were performed with equipment of *the National Infrastructure INFRAMAT (Д01-155/28.08.2018),* granted by the Bulgarian Ministry of Education and Science.

References

1. J. Lucas, P. Lucas, T. Le Mercier, A. Rollat and W. Davenport Rare Earths: Science, Technology, Production and Use, Elsevier Inc., (2014), Radarweg 29, PO Box 211, 1000 AE Amsterdam, Netherlands.
2. B. Sakintuna, F. Lamari-Darkrim, M. Hirscher, *Int. J. Hydrogen Energy*, 32 (2007) 1121.
3. M. Spodaryk, L. Shcherbakova, A. Sameljuk, A. Wichser, V. Zakaznova-Herzog, M. Holzer, B. Braem, O. Khyzhun, Ph. Mauron, A. Remhof, Y. Solonin and A. Züttel, *J. Alloys Compd*., 621 (2015) 225.
4. G. D. Adzic, J. R. Johnson, J. J. Reilly, J. McBreen, S. Mukerjee, M. P. Sridhar Kumar, W. Zhang and S. Srinivasan, *J. Electrochem. Soc*., 142 (1995) 3429.
5. F. Liang, J. Lin, Y. Cheng, D. Yin, Y. Wu and L. Wang, *Sci. China Technol. Sci*., 61 (2018) 1309.
6. D. Endo and E. Akiba, *Mater. Trans., JIM*, 47 (2006) 1914.
7. L. Grinberga and J. Kleperis, Advances in Composite Materials, IntechOpen, (2011) Available from:https://www.intechopen.com/books/advances-in-composite-materials-for-medicine-and-nanotechnology/composite-nanomaterials-for-hydrogen-technologies
8. E. Anil Kumar, M. Prakash Maiya, S. Srinivasa Murthy and B. Viswanathan, *J. Alloys Compd*., 476 (2009) 92.
9. S. Srivastava and K. Panwar, *Mater. Renewable Sustainable Energy*, 4 (2015) 19.
10. X. Shan, J. H. Payer and W. D. Jennings, *Int. J. Hydrogen Energy*, 34 (2009) 363.
11. M. R. Esquivel and G. Meyer. *Mater. Sci. Forum*, 570 (2008) 72.
12. S. Srivastava and K. Panwar, *Mater. Res Bull*., 73 (2016) 284.
13. St. Todorova, V. Rangelova, V. Koleva and T. Spassov, J. Nanomater., 2019, Article ID 6258484.
14. M. Okumura, A. Ikado, Y. Saito, H. Aoki, T. Miura and Y. Kawakami, *Int. J. Hydrogen Energy*, 37 (2012) 10715.
15. M. Gao, S. Zhang, H. Miao, Y. Liu and H. Pan, *J. Alloys Compd*., 489 (2010) 552.
16. M. Spodaryk, L. Shcherbakova, A. Sameljuk, A. Wichser, V. Zakaznova-Herzog, M. Holzer, B. Braem, O. Khyzhun, Ph. Mauron, A. Remhof , Y. Solonin and A. Zuettel, *J. Alloys Compd*., 621 (2015) 225.
17. Z. Zhu, S. Zhu, H. Lu, J. Wu, K. Yan, H. Cheng and J. Liu, *Int. J. Hydrogen Energy*, 44 (2019) 15159.
18. K. Goto, T. Hirata, I. Yamamoto and W. Nakao, *Molecules*, 24 (2019) 2420.
19. J. Qu, B. Sun, J. Zheng, R. Yang, Y. Wang and X. Li, *J. Power Sources*, 195 (2010) 1190.
20. J. Cao, H. Xie, Zh. Wen, G. Cao , L. Ji , Y. Fan and B. Liu, *Int. J. Electrochem. Sci*., 12 (2017) 5854.
21. X. Yuan, Z.-F. Ma,Y. Nuli and N. Xu, *J. Alloys Compd*., 385 (2004) 90.
22. H.-S. Kim, M. Nishizawa and I. Uchida, *Electrochim. Acta*, 45 (1999) 483.
23. J. Chen, S.X. Dou, D.H. Bradhurst and H.K. Liu, *Int. J. Hydrogen Energy*, 23 (1998) 177.
24. G. Zheng, B.N. Popov and R.E. White, *J. Electrochem. Soc*., 143 (1996) 834.
25. B. Zhang, H. Liu, X. Jing, Y. Ning and Xiaoqiang Han, *Int. J. Hydrogen Energy*, 43 (2018) 22427.

26. G. Zheng, B. N. Popov and R. E. White, *J. Electrochem. Soc*., 142 (1995) 2695.